ADVANCED MATERIALS TECHNOLOGIES
www.advmattechnol.de

Room Temperature Electronic Functionalization of Thermally Sensitive Substrates by Inkjet Printing of a Reactive Silver-Based MOD Ink

Ye Zhou, Zongpu Xu, Hao Bai, and Caroline E. Knapp**

The developments in inkjet printing technology and the printed electronics industry in the past two decades have provided cost-effective, environment-friendly, and reliable alternates to traditional methods of fabricating electrical devices. However, most commercial metallic inks require high sintering temperatures to form desired functional patterns, which limits the applications of printed electronics in scenarios that require electrical devices on thermally sensitive substrates, like biomaterials or bio-synthetic composite materials. This study has provided the synthetic route of a novel silver-based metal organic decomposition (MOD) ink which has been used to form highly conductive silver films on the thermally sensitive skin-inspired silk/epoxy composite substrates by directly inkjet printing with accurate pattern control, whilst self-decomposing and sintering at room temperature. The fabricated silver patterns on the thermally sensitive silk/epoxy composite substrate were highly conductive with conductivity of 4.65×10^4 S m^{-1}. These silver patterns also showed impressive malleability as bulk silver films, which could be further developed into motion sensors for wearable devices or medical applications. Our strategy provides a general platform for electronic functionalization without temperature constraints. The particle-free, reactive silver-precursor, and lower sintering temperature of the ink also widen the choices of substrates, as exemplified herein with outstanding printing quality and high electrical conductivity (1.20×10^6 S m^{-1}) also achieved on paper.

1. Introduction

With the increasing environmental concerns of electronic waste (E-waste),[1] inkjet printing technology, "borrowed" from the graphic media industry was adapted in principle to the production of large volume flexible electronics to replace the traditional integrated circuits manufacturing, to simplifying manufacture processes, decreasing costs, and minimizing waste generation. In 2000, researchers at the University of Cambridge made a fully printed organic transistor via inkjet printing.[2,3] Due to the development of nanoscale inorganic materials in the past few years, metallic nanoparticles, especially silver and copper nanoparticles, were made into inks for printed electronics.[4–7] Since the advent of nanoparticle-based inks, metal-organic decomposition (MOD) inks, a novel type of ink for metal deposition, has become popular in research.[8] MOD inks offer an alternative to their nanoparticle-based counterparts, existing as solutions of metal precursors formulated specifically for printing. The formulation of these inks is central metal cations, bound to ligands that can be reduced to metal atoms and the cleaved ligand molecules removed via certain initiations, like thermal, plasma, or even laser sintering[9–12] thus finally forming aggregated metallic patterns on substrates. In comparison with nanoparticle inks, there are no suspended particles in MOD inks, which means the inks can be printed smoothly through nozzles with accurate droplet control, thus avoiding clogging.[13]

Among commercial metals, silver has the lowest bulk electrical resistivity (1.59 $\mu\Omega$cm)[14] and in comparison with other excellent conductors, e.g. copper and aluminum, silver has a relative high redox potential,[15] the reduction of silver cations to metallic silver could be very fast without middle products, which allows silver based precursors to be directly printed and sintered under standard atmospheric conditions while copper or aluminum precursors normally need to be deposited and sintered under the protection of nitrogen gas or vacuum to avoid oxidation to metal oxides or hydroxides.[16,17] Hence from 2005, a range of silver carboxylate and diketonate complexes have been developed into silver MOD-based inks,[18–20] which

Y. Zhou, C. E. Knapp
Department of Chemistry
University College London
20 Gordon Street, London WC1H 0AJ, UK
E-mail: caroline.knapp@ucl.ac.uk
Z. Xu
Institute of Applied Bioresources
College of Animal Sciences
Zhejiang University
Hangzhou 310058, China
H. Bai
State Key Laboratory of Chemical Engineering
College of Chemical and Biological Engineering
Zhejiang University
Hangzhou 310027, China
E-mail: hbai@zju.edu.cn
The ORCID identification number(s) for the author(s) of this article can be found under https://doi.org/10.1002/admt.202201557.

DOI: 10.1002/admt.202201557

could be inkjet-printed to form conductive silver patterns on a wide range of substrates including glass, papers, and polymers (PET, PI, etc.). However, sintering temperatures for these inks still vastly exceed 100 °C because of the addition of humectant additives and binders to improve their wettability and adhesions on substrates. With the recent development of wearable devices for deep-tissue sensing,[21] and electronic skins,[22,23] future electronics based on biomaterials or biosynthetic composite materials and even human skin highlight an urgent need for sub 100 °C fabricating processes. As mentioned before, silver has a high redox potential and so providing a precursor is active enough to start decomposing as soon as being deposited onto a substrate, the generated small silver particles could act as the seeds and fixed points of crystallization of metallic silver, in which case, humectant additives and binders may not be necessary, and the sintering temperature of silver MOD based inks could be considerably lower. In 2012, Walker et al. deposited highly conductive metallic silver tracks onto glass and ethylene-vinyl acetate substrates at 90 °C for 15 min with a silver-based MOD precursor $[Ag(NH_3)_2]^+[C_2H_3O_2]^-$.[24] This precursor was synthesized from the reaction of silver acetate with ammonium hydroxide and formic acid. The deposited silver tracks from the decomposition of this precursor achieved conductivity equivalent to that of the bulk silver. It is worth noting that this silver MOD-based precursor could also form conductive silver film with some silver acetate still remaining when sintered at room temperature for over 24 hours. The molecular structure of this kind of silver MOD-based precursor is stabilized through dative interactions between the lone pair of electrons on the nitrogen of the aminoalcohol and the central metal ion. The amine coordinates with silver acetate and eventually forms a diamminesilver(I) complex. Vaseem et al. made a modification of the formulation using 2-aminoethan-1-ol (EA) to replace ammonium hydroxide to increase the long-term stability of the precursor,[25] however the temperatures required for this ink to sinter metallic silver tracks were higher than Walker et al.'s precursor and the conductivities were also relatively lower. Bhat et al. improved Vaseem et al.'s precursor by adding 2% hydroxyethyl cellulose as viscosifier, dispenser, and adhesion promotor to enhance and maintain the dispersion and viscosity of the ink.[26] This type of ink could be printed and form conductive features on PET and PI substrates with remarkable conductivities (10^6–10^7 S m^{-1}), which was compatible to bulk silver after sintering at 70–100 °C.

1-aminopropan-2-ol (AP), as another alkanolamine with similar chemical structure to 2-aminoethan-1-ol (EA), could also be employed to form a diamminesilver(I) complex with silver acetate. The silver-based precursor synthesized by AP might be more reactive and have lower decomposing temperature than that synthesized by EA. Tinker et al. synthesized and compared EA and AP-based precursors in their study.[27] Both precursors could decompose into elemental Ag with similar particle size, but their Oxygen Reduction Reaction (ORR) activities showed that the onset potential of the AP precursor was higher than that of the EA precursor. It was reported that the relative pKa values of the respective alkanolamine might positively affect their binding abilities and influence the variation of onset potential from linker to linker. The pKa of AP is 15.3, which is much higher than that of EA (pKa: EA = 9.5), hence AP may facilitate easier tethering to Ag cations.

Xu et al. in 2020 fabricated a novel polymer and fiber composite films, which were skin-inspired and produced by epoxy polymer infiltration of flat silk cocoon fibers. The great flexibility, transparency, and outstanding tear resistance make it an excellent supporting substrate in electronic skin devices.[28] However, as an epoxy resin-based material, this type of composite films is thermally sensitive due to the low glass transition temperature (T_g) of 80 °C rendering further functionalization impossible at temperatures >100 °C. The liquid and vapor permeability of these films, which depending on the fill rate of epoxy resins, are also significantly relative to temperature. When the temperature of the film is lower than T_g, the liquid water permeability will increase with the increase in temperature. If the temperature continues rising over T_s, the liquid permeability will start to decrease.[29] To directly deposit conductive patterns on the surface of such substrates through inkjet printing, the processing temperature needs to be controlled to as low a value as possible to suppress the functionality losses of substrates. Herein we exploit the high reactivity of Ag-AP-based MOD precursor, and report herein its decomposition to metallic silver at low temperatures. The ink synthesized based on this precursor can be used to form conductive silver metal patterns (conductivity >10^5 S m^{-1}) on this thermally sensitive silk/epoxy composited film substrate by directly inkjet printing and sintered at room temperature. Meanwhile, the potential for particle-free and low sintering temperature inks have enabled a wider range of choices of unconventional substrates, such as paper or fiber materials for printed electronics. Silver patterns on paper with outstanding printing quality and high electrical conductivity of 1.20×10^6 S m^{-1} were also fabricated in this study.

2. Results and Discussion

In this study, as presented in the schematic shown in **Figure 1**a, the silver-based MOD precursor was synthesized through complexation between silver acetate and 1-aminopropan-2-ol (AP). It is proposed that the lone pair of electrons on the nitrogen of AP coordinates with the metallic cation from silver acetate and forms a diamminesilver(I) complex. When the diamminesilver(I) complex begins to decompose, the freed silver ions will be reduced to silver metal by formate anions. No humectant additives were added during the mixing process with the exception of ethanol to adjust the surface tension to 32.27 mN m^{-1}, to make it into an inkjet printable ink (Figure S2, Supporting Information).

When AP was mixed with silver acetate, the solution became a translucent light brown color. It was hypothesized that this brown coloration is caused by the formation of silver oxide from any remaining reagent that had not converted to the diamminesilver(I) complex due to the lack of anions in solution.[24] We propose that upon formation of the silver oxide particles, as the formic acid is slowly added, this reagent dissolves the silver oxide (evidenced by a color change) which in turn encourages the lone pair on the nitrogen of AP to coordinate with silver cations. This results in the desired

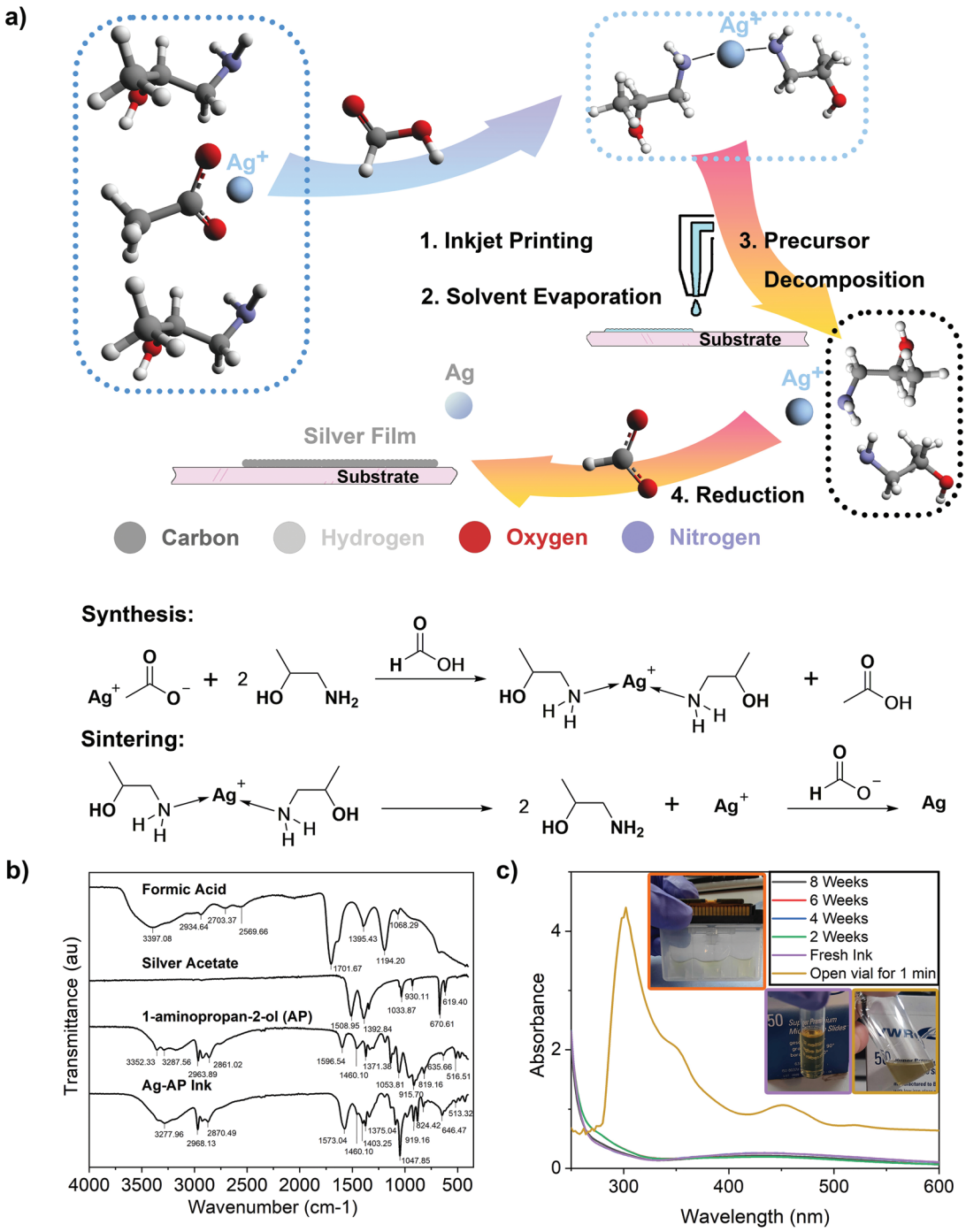

Figure 1. Overview of the process: a) Synthesis and decomposition reactions of the Ag-AP-based MOD precursor. b) The FT-IR spectra of formic acid, silver acetate, 1-aminopropan-2-ol (AP), and synthesized Ag-AP ink. c) The stacked UV-vis spectra of the freshly prepared ink, the ink stored for 2, 4, 6, 8, and the ink exposed to air for 1 min. Inset: pictures of the fresh ink loaded in printer cartridge (orange box), freshly synthesized ink (purple box), and the ink exposed to air for 1 minute (brown box).

diamminesilver(I) complex balanced with formate anions. As the effective reducing agent for the decomposition and reduction of the resultant deposited ink, the amount of formic acid added will positively affect the formation speed of metal silver, however, formic acid could also react with silver acetate to form silver metal precipitates and acetic acid, which would decrease the loading amount of silver in the ink and is therefore undesirable. Hence the amount of formic acid added during the formulation of inks had to be controlled to reach the requirements that all the silver-containing reagent would be fully converted to the diamminesilver(I) complex, such that the ink remained kept its relatively high silver loading.

PXRD confirmed that any silver oxide present in the formulation had dissolved as only the observed diffraction peaks for filtered precipitates were indexed to face-centered cubic silver structure (ICSD:44387) and no phase of silver oxide was detected (S3, Supporting Information).

The interactions between silver ions and AP were investigated through FTIR spectroscopy. As shown in Figure 1b, FTIR spectra of chemicals used for synthesis, including formic acid, silver acetate, and AP, were measured along with the spectra of synthesized Ag-AP ink. The transmittance peak at 1702 cm^{-1} of pure formic acid, associated with an aldehyde group (H–C=O), was not found in the IR spectra of Ag-AP ink at all. This was further supported by the high pH value of the Ag-AP (11.42 at 23 °C) (Figure S6, Supporting Information), indicating that the formic acid was fully reacted and neutralized with silver acetate and excess AP.

The IR spectra of the Ag-AP ink contained peaks in similar positions to those in the spectra of silver acetate and AP. Compared with the spectra of pure AP, the peak of in-plane bending of the NH group at 1460 cm^{-1} became weaker, while the O–C–C in-plane bending vibration at 635 cm^{-1} became stronger. In addition, a new COO- symmetrical stretching vibration peak showed at 1403 cm^{-1}. These differences indicated that the AP has changed its coordination resulting in a shift in wavenumber as it coordinates to the silver ions to from a diamminesilver(I) complex.

The resulting ink once loaded into a printer cartridge, as shown in Figure 1c, is visibly particle-free and transparent. The synthesized ink was sealed and stored in fridge for over 8 weeks and undertook UV-vis measurements every two weeks. The peak of silver nanoparticles is typically at the wavelength of 425 nm.[26] For all the tested samples, no absorbance spectra peaks were detected after the wavelength of 300 nm. But when the ink was exposed to air, as evaporation occurs, silver nanoparticles started to form. It is estimated that although the synthesized ink is designed to be reactive, with proper storage conditions to prevent the evaporation and decomposition, it has been shown to have a long shelf life.

For the resulting ink, the maximum silver content was limited by the solubility of the diamminesilver(I) cation in solution. The synthesized ink was composed of 12.56 wt. % silver according to the thermogravimetric analysis (TGA) as shown in **Figure 2**a, while the calculated and predicted silver concentration was 13.80 wt.%. The heat flow had a sudden drop at 160 °C, which was close to the boiling point of AP (Boiling point: AP = 159.46 °C). The rapid evaporation of solvent accelerated the decomposing of the precursor. To investigate if this precursor could still decompose to metallic silver, due to evaporation at lower temperatures, we made a further thermogravimetric analysis, as shown in Figure 2b, whereby the ink was heated up from 30 to 80 °C (Boiling point: Ethanol = 78.37 °C) under N_2 flow protection and held for 10 h until the solid residue weight decreased to 12.56 wt.%. It is indirectly indicated that this precursor might self-decompose to metallic silver at temperature much lower than the boiling point of the solvent.

Initially, to investigate various sintering conditions of the synthesized ink, and decomposition of the precursor at different temperatures, five samples were prepared by inkjet printing on glass substrates and sintering at 23 (RT), 50, 80, 120, and 150 °C (Figure S7, Supporting Information).

According to the film XRD analysis in Figure 2c, well crystallized metallic silver phase was detected in all the samples. Upon sintering over 80 °C, elemental silver was the only phase that remained. A weak peak closed to an angle of 30° was detected both at the samples sintered at room temperature and 50 °C. The films on the sample sintered at room temperature were scraped and ground into powder for further powder XRD analysis. As shown in Figure 2d, peaks marked with asterisks are likely corresponding to residual acetate groups.[30] The surface characterization and chemical composition of these films on glass slides were identified by SEM and EDS surface energy and point spectra. As SEM images shown in Figure 2e, with the sintering temperature increasing over 80 °C, no visible organic residues were observed or detected, while amorphous organic residue existed and filled gaps among crystallized silver particles and clusters on the sample sintered at room temperature. Ag and C were detected by EDS spectra (Figure 2f), with the films sintered at room temperature still exhibiting a good electrical conductivity of 4.65×10^4 S m^{-1} (Figure S8, Supporting Information). At low sintering temperature, due to the long sintering duration, the residual acetate groups in solution might form a small amount of silver acetate with Ag^+ ions, which lose the protection from diamine ligands and therefore do not reduce to metallic silver during the long sintering process.[31] The formation of the silver acetate could be alleviated or avoided through decreasing the sintering duration by droplet control of inkjet printing and assistance of vacuum evaporation. (Figure S10, Supporting Information)

To investigate whether this new strategy could aid in the functionalization of thermally sensitive substrates, the synthesized Ag-AP ink was then printed onto silk/epoxy composite films and sintered at 23 (RT), 80, 120, and 150 °C respectively (Figure S13, Supporting Information). The surface morphologies of printed patterns were characterized by GIXRD, AFM, and SEM. As the film GIXRD measurements shown in **Figure 3**a, metallic silver phase was the only crystalline phase detected on the samples sintered at room temperature 23, 120 and 150 °C while no metallic silver phase was detected on the surface of the sample sintered at 80 °C. According to the AFM profiles in Figure 3b, there was no silver films detected on the surface of the sample sintered at 80 °C. The silver film of the sample sintered at room temperature had the lowest surface roughness, indicating a better surface morphology. The R.M.S roughness of surfaces of printed patterns was 86.29, 23.9, 216.4, and 152.5 nm for the samples sintered at room temperature 23, 80, 120, and 150 °C, respectively (S10).

As the SEM images show in Figure 3c, uniform and continuous films composed of well-crystallized silver were observed on the samples sintered at room temperature. On samples sintered at 80 °C, silver particles, and clusters formed inside substrate and under the surface layer while no silver particles were observed on the surface. On the sample sintered at 120 °C, silver particles and clusters were inlayed on the surface of the substrate. On the sample sintered at 150 °C, the silver film was formed on the surface of the substrate but with higher roughness, compared with the sample sintered at room temperature.

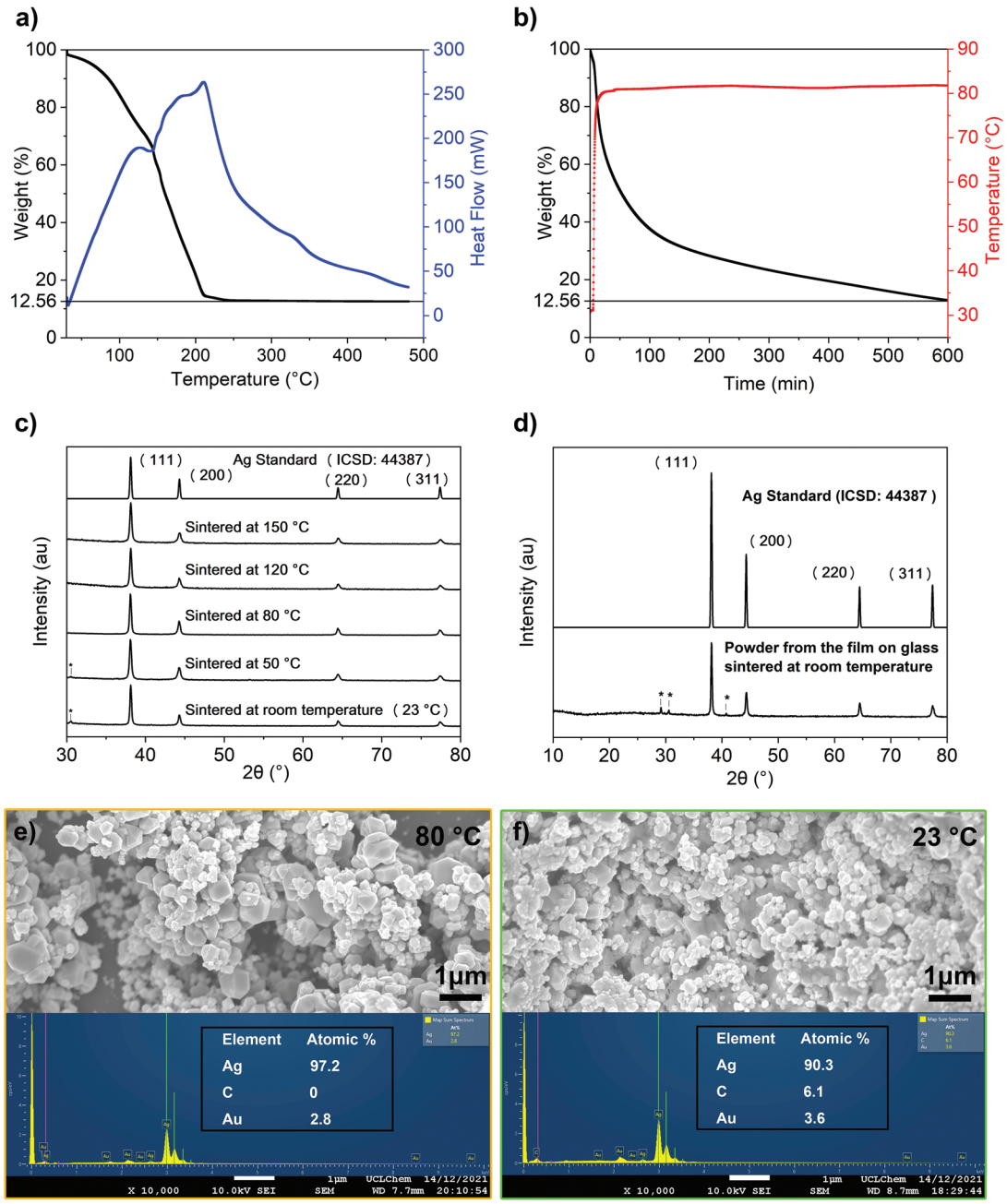

Figure 2. a) TGA curve of synthesized Ag-AP ink heated from 30 to 500 °C in N_2 and b) Ag-AP ink heated from 30 to 80 °C and held for 10 h in N_2. c) Grazing incidence X-ray diffraction (GIXRD) analysis of patterns of inkjet-printed Ag-AP ink on glass and sintered at 23 (RT), 50, 80, 120, and 150 °C, respectively. d) Powder XRD analysis of the inkjet-printed films on glass, sintered at room temperature (asterisks denoted peaks are assigned to silver acetate). SEM images and EDS spectra of inkjet-printed Ag-AP ink on glass slides and sintered at e) 80 °C and f) room temperature. Au in EDS analysis is from the Au sputtering coating for SEM and should be negligible in this study.

As mentioned previously, the liquid permeability of thermally sensitive tear-resistant silk/epoxy composite substrates are affected by temperature. According to the characterization of surface morphologies reported here, we may conclude a general deposition and sintering model of the Ag-AP ink on silk/epoxy composite film substrates, as the illustration shows in **Figure 4**a: after ink droplets are printed onto the substrates, solvent evaporation and ink penetration due to the permeability of the epoxy polymer start at the same time. Therefore, the evaporation and penetration rates will both relative to the sintering temperature. Silver particles and clusters begin to generate in the liquid phase due to evaporation and grow along the silk fibers inside the substrates due to the capillary absorption.[32]

To ensure the low sintering temperature of the ink, there were no additives or binder solvents added to prevent the spreading of the deposited ink on substrate surface,[33,34]

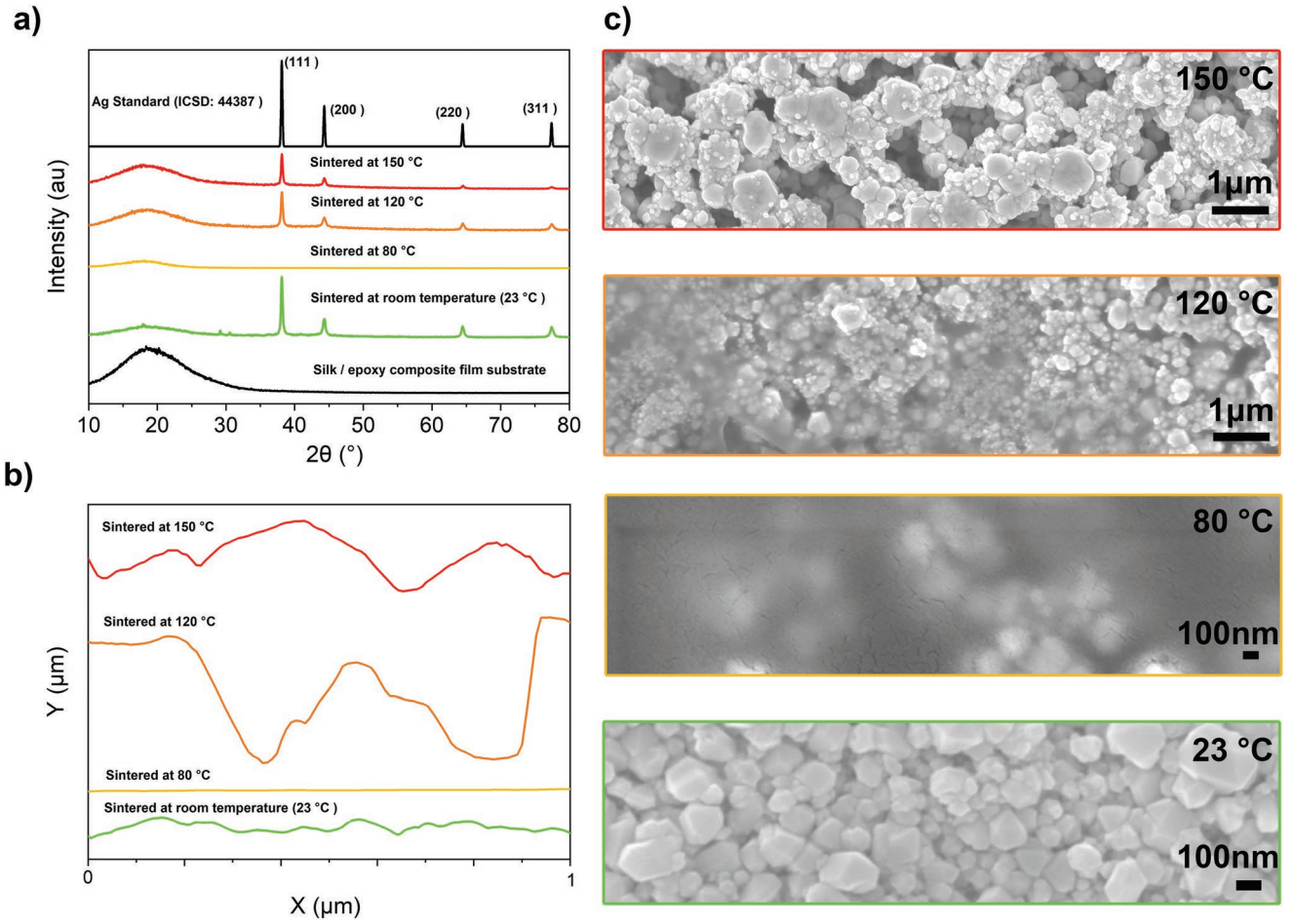

Figure 3. a) Grazing incidence X-ray diffraction (GIXRD) analysis and b) atomic force microscopy (AFM) profiles, and c) SEM images of patterns of inkjet-printed Ag-AP ink on silk/epoxy composite film substrates and sintered at 23 (RT), 80, 120, and 150 °C, respectively.

which made the shape and resolution control of printed patterns a significant challenge.[35] The spreading of the liquid droplet deposited on the substrate could be observed through the change of the contact angle. It has been shown previously that the –OH group of AP and the added ethanol made the ink extremely wettable on the epoxy polymer surface[36] with an initial contact angle of 24.5°. The deposited ink would spread on the epoxy polymer surface quickly in the absence of any restrictions.[37] In the work presented herein the contact angle change of the Ag-AP ink versus an AP solution droplet on the thermally sensitive silk/epoxy composite substrates are different, as shown in Figure 4b,c. After ≈30 min, the contact angle of the Ag-AP ink droplet on the substrate only changed from 24.5° to 16.8° while that of the AP solution droplet changed from 23.7° to 3.7°. For the Ag-AP ink synthesized in this study, as soon as it is deposited, the silver particulates would firstly generate along the edge of the pattern because of the high reactivity of the Ag-AP precursor and internal flow inside the liquid phase of deposited ink and have therefore acted to restrict the spreading of ink[38,39] on the substrate, fortuitously this effect has aided in ensuring the size and shape accuracy of the printed pattern in the absence of humectant additives.

As mentioned before, the tear-resistant silk/epoxy composite substrates used in this study were liquid permeable and the permeability could be affected by temperature. The glass transition temperature of the tear-resistant silk/epoxy composite substrate is ≈80 °C. When the sintering temperature was lower than 80 °C (T_g), both evaporation and penetration rates will increase relative to temperature. However, when the sintering temperature was higher than T_g, the evaporation rate would increase whilst the penetration rate began to decrease, with increasing temperatures. Hence the position where silver nanoparticles are formed can be directly tuned to process temperature, such that the amount of silver particles formed either in the liquid phase or inside the composite substrates can be varied, eventually affecting the film formation and resultant conductivity/functionality. Diamminesilver (I) complex is only able to exist in solution and will start to decompose as soon as solvent consumed for whatever reason. The cellulose fiber structures may also cause the decomposition from the bottom of deposition but not only the decomposition from the top caused by evaporation.[32,40,41] Ideally, the silver particles most penetrated into the composite would grow and stack upwards to break the surface and connect with silver particles and clusters generated in liquid phase to form continuous and conductive silver films.

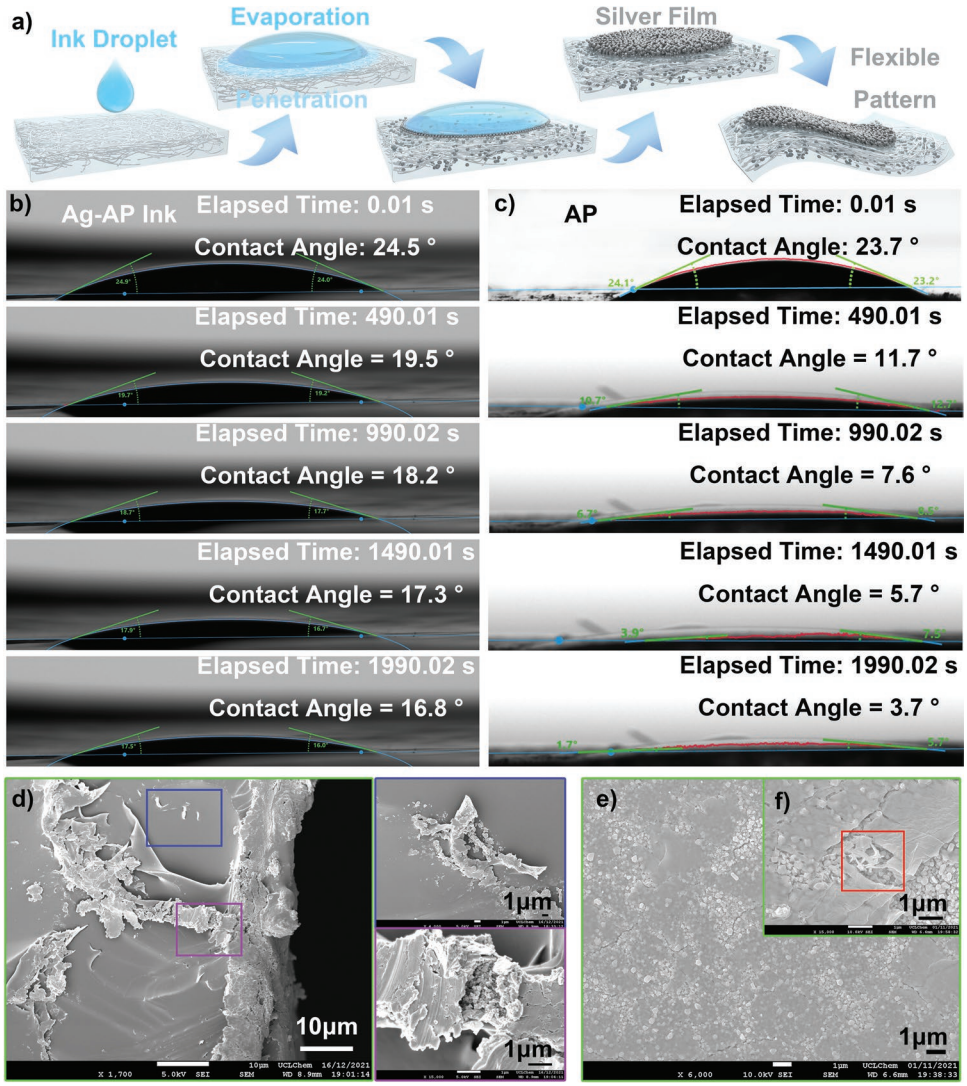

Figure 4. a) Schematic illustration of deposition and sintering process of Ag-AP inks on thermally sensitive silk/epoxy composite substrates. b) Contact angle change of the Ag-AP ink droplet on the thermally sensitive silk/epoxy composite film, from 24.5° to 16.8° in 1990.2 s. c) Contact angle change of the AP solution droplet on the thermally sensitive silk/epoxy composite film, from 23.7° to 3.7° in 1990.2 s. d) High magnitude cross-section SEM images of inkjet-printed Ag-AP ink on thermally sensitive silk/epoxy composite film with high printing resolution and sintered at room temperature. Dark blue box highlights the silver nanoparticles attached to the silk fiber tail away from the printed surface. The purple box highlights the silver nanoparticles formed inside the silk cellulose fiber structures. e,f) SEM images of inkjet-printed Ag-AP ink on thermally sensitive silk/epoxy composite substrates with low printing resolution and sintered at room temperature. The red box highlights the silk fibres brought out by the growth of silver particles.

According to the cross-section SEM images shown in Figure 4b, silver particles from penetrated ink generated along silk fibers (Figure 4c), fully filled the gaps and vacancies of the silk fiber structures (Figure 4d) and connected with the silver film formed upon the surface. As the SEM images show in Figure 4e,f, we controlled the ink depositing density via lower printing resolution, to investigate the growth of silver particles from the ink penetrating the substrates and their effects on substrate surfaces. The growing silver particles and clusters inside the substrates are stacked upwards to break the surface.

Hence, for the samples sintered at 80 °C, the high liquid permeability of the substrate and relatively low evaporation rate allowed most of the deposited ink to penetrate into the substrates before beginning its decomposition into silver particles: a process driven by the impregnation of ink into the silk fibers. At the sintering temperature of 120 °C, liquid permeability decreased while the evaporation rate increased, the lower penetration depth of ink allowed some of the silver particles formed inside the substrate to break the surface and connect with particles formed above the surface but still failed to form a continuous silver film. When sintering temperature rose to 150 °C, the evaporation rate was in domination of generating silver particles, such that large silver particles and clusters grew upon the surface of substrate. However, the rapid evaporation and gas generation due to decomposition of the ink resulted in large vacancies.

For the samples sintered at room temperature, low evaporation rate allowed the ink to penetrate downward into the substrate,

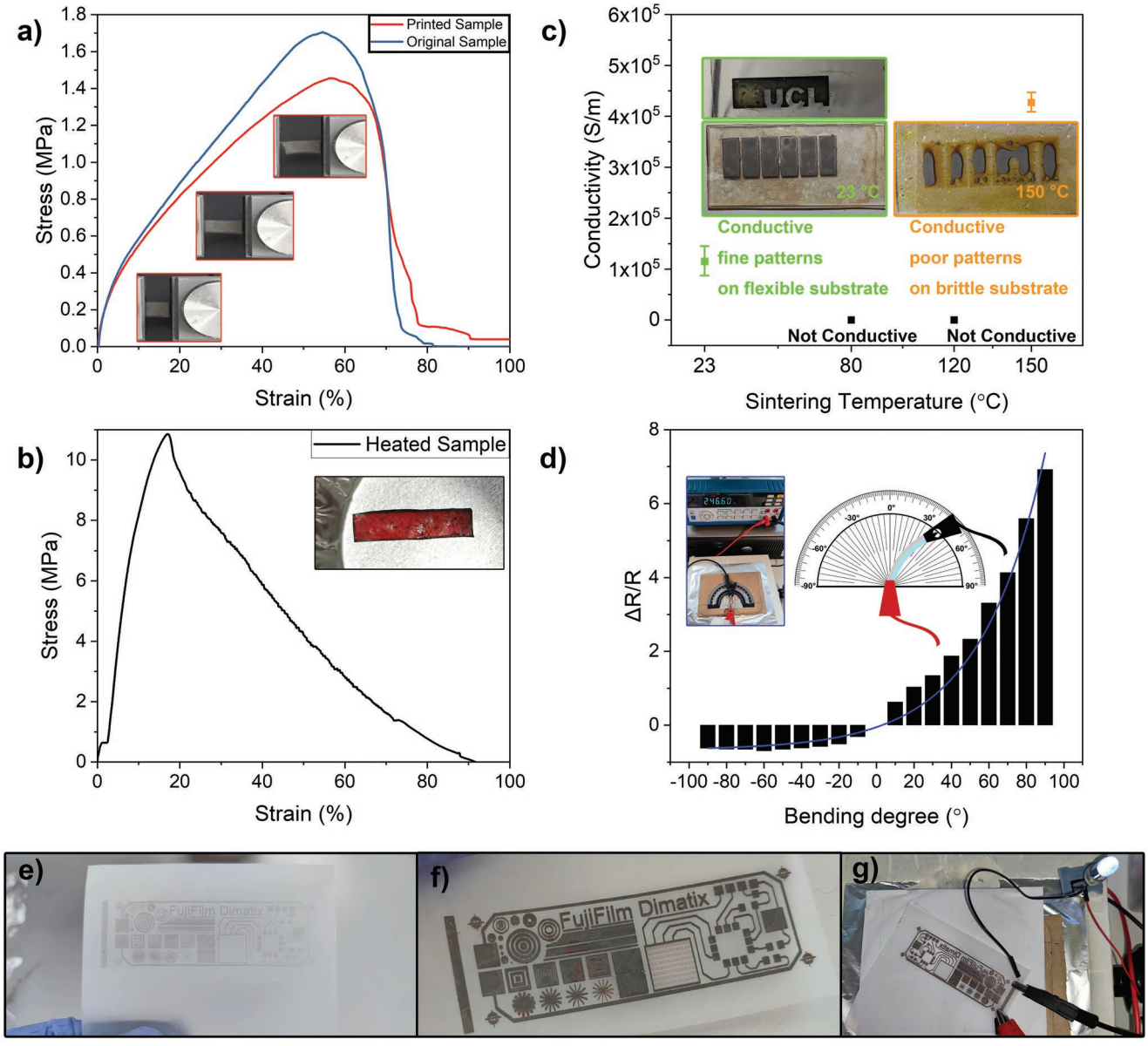

Figure 5. a) Stress–strain curves of the original silk/epoxy composite substrate sample and the inkjet-printed sample of Ag-AP ink on silk/epoxy composite substrate (sintered at room temperature) with photos of the test inset. b) Stress–strain curve of heated silk/epoxy composite substrate sample at 250 °C for 2 h. c) The conductivity of inkjet-printed patterns on silk/epoxy composite substrates and sintered at room temperature 23, 80, 120, and 150 °C, respectively. d) Resistance-bending test of inkjet-printed patterns on silk/epoxy composite substrates and sintered at room temperature (23 °C). e) Inkjet-printed patterns on paper substrates with synthesized Ag-AP ink and f,g) sintered at 80 °C.

whilst the suitable liquid permeability of the substrate limited the depth of ink penetration before the formation of silver particles due to the solvent absorption by silk fibers. This eventually formed well-shaped silver patterns on the surface (Figure S11, Supporting Information).

As mentioned previously the silk/epoxy composite substrate material has outstanding tear resistance with great flexibility but is also sensitive to heat. As the stress-strain curve and photograph are shown in **Figure 5**b, after heat treatment at 250 °C for 2 h, the substrate material became brittle and brown in color and lost the desired functionality. The synthesized Ag-AP ink in this study is capable of being inkjet-printed on the silk/epoxy composite substate and sintering into conductive silver films at room temperature. As the stretching test shows in Figure 5a, the printed sample kept its excellent mechanical performance, with a similar profile as the original silk/epoxy composite substrate. The samples sintered at room temperature and 150°C were electrically conductive (Figure 5c), with conductivity of 1.15×10^5 and 4.27×10^5 S m^{-1}, respectively. The samples sintered at 150 °C had better conductivity performance because of larger silver clusters on the film surface, but the high sintering temperature and rapid evaporation restricted the formation of desired patterns and destroyed the thermally sensitive silk/epoxy composite substrates.

Bending test studies were undertaken to prove that after inkjet-printing and sintering at room temperature, the reduced silver nanoparticles had strongly connected to each other and formed a continuous silver film, which could display the malleability of bulk silver metal, as a continuous material, not as powders or separated islands. The bending test (SI), as shown in Figure 5d, shows that the resistivity of printed patterns changed smoothly with the bending degree and kept conductive in the bending range from −90 ° to 90 °. The sensitive resistance responses to bending indicate that these fabricated conductive inkjet-printed patterns, using the Ag-AP MOD ink, on the silk/epoxy composite substrates with outstanding tear resistance have huge potential and are worthy of further development[30,31] into motion sensors for wearable devices or electrical skins. For different substrates with different wetting properties, the printing setting and sintering conditions should always be specially optimized for the certain circumstance. None-the-less the high reactivity and lower requirement for sintering temperature of the synthesized Ag-AP ink in this study provides a wider range of choices of untraditional thermally sensitive substrates for printed electronics. This of course also applies to substrates as common as paper as we have shown in Figure 5e,f,g, a conductive (1.20×10^6 S m^{-1}) electric circuit pattern with impressive complexity and resolution was printed on paper and sintered at 80 °C (Figure S11, Supporting Information).

3. Conclusion

In this study, we provide a unique room-temperature electronic functionalization strategy to thermally sensitive substrates. Through a novel chemical synthesis route of silver-based metal-organic decomposition (MOD) ink, and the combination effect of ink penetration, evaporation, and capillary effects of silk fibers, conductive silver films (conductivity > 10^5 S m^{-1}) with fine pattern quality were formed on the sample inkjet-printed with high printing resolution and sintered at room temperature which represents a potential breakthrough for this field. The fabricated silver pattern on this flexible substrate can be widely applied in areas of wearable devices or electrical skins, such as the bending motion sensor presented in this study. The silk/epoxy composite material used in this study has outstanding flexibility, transparency, and tear resistance and shows great potential to be applied as substrates for wearable devices or electrical skins. However, as a type of thermally sensitive silk/epoxy composite substrate with tricky liquid permeability, the sintering temperature of ink deposited on silk/epoxy composited film substrate needs to be limited to under 80 °C, and as low as possible, to avoid the functionality loss of substrates. An Ag-based MOD ink for inkjet printing was synthesized by dissolving silver acetate into 1-aminopropan-2-ol (AP). Through adjusting silver content by formic acid and surface tension control with ethanol, this novel MOD precursor was made into an inkjet printable humectant-free Ag-AP MOD-based ink, which could decompose to metallic silver particles and form electrically conductive films with the designed pattern on substrates through droplet control by inkjet printing and sintering at low temperature. The synthesized Ag-AP ink was deposited on glass slides and sintered at room temperature (23 °C), formed silver patterns with electrical conductivity of 4.65×10^4 S m^{-1}. The capability of low-temperature decomposition of the synthesized ink made it possible to directly fabricate conductive silver patterns on a wider range of substrates via inkjet printing. In addition, as a MOD ink without any additives or benders, the particle-free feature, and the low sintering temperature, and of the synthesized ink made it possible to fabricate conductive patterns on unconventional fiber substrates of printed electronics. To showcase this feature, silver patterns with outstanding printing quality and high electrical conductivity of 1.20×10^6 S m^{-1} were also printed onto paper.

4. Experimental Section

Materials: The silk/epoxy composite films were fabricated and provided by Dr. Zongpu Xu. Silver (I) acetate (anhydrous) (99wt. %) was purchased from Alfa Aesar. 1-aminopropan-2-ol (AP) (93vol.%) was supplied and purchased from Sigma–Aldrich. Formic acid (≥95vol.%) was purchased from Sigma–Aldrich. The prototype commercial particle-free ink was supplied by HS Electronics. HS Electronics Co., Ltd., China.

Synthesis of Ag-AP MOD Precursor: The mixing procedure during the synthesis was operated under the condition of ice-bath, with a temperature of 0–3 °C. Silver(I) acetate (0.5 g, 12 mmol) was vortex-mixed with Ethanol (1 mL, 0.8 g) in a vial for 30 s and form white homogeneous suspension. 1-aminopropan-2-ol (1 mL, 0.973 g, 13 mmol) was vortex-mixed with the suspension for 120 s, resulted in translucent light brown color solution with small amount of dispersed black precipitates. Formic acid (0.05 mL, 0.061g, 1.2 mmol) was dropwise added and the solution was vortex mixed after the addition of every drop. The vial was sealed and wrapped with aluminum foil after the mixing procedure. The solution in the vial was left to be kept stirring overnight at room temperature (23 °C), after which it was filtered through a 200 nm syringe filter to yield a clear and transparent Ag-AP precursor. The black precipitates left in filters were collected, washed with ethanol, and dried at 80 °C for 3 h.

Preparation of Metal Silver Film Deposition on Glass Slides: To evaluate the decomposition and nanoparticle growth process of the ink, five groups of samples on glass slides were prepared by inkjet printing and thermal sintering at different temperatures. Each group contained six samples. Before printing, surfaces of glass slides were wiped cleaned by acetone and undertaken plasma surface treatment (HENNIKER HPT – 100, 100% power) for 10 min. The designed pattern was inkjet-printed with high printing resolution (2540 DPI) on pr-treated glass substrates and thermal sintered at room temperature for 12 h in vacuum evaporation chamber, 50 °C for 3 h in oven, 80 °C for 2 h in oven, 120 °C for 2 h in oven and 150 °C for 1 h in oven, respectively, to ensure the printed samples were fully dried.

Preparation of Metal Silver Film Deposition on Flat Silk Cocoon and Epoxy Resin Composite Films (Silk/Epoxy Composite Films): Eight groups of samples on silk/epoxy composite film substrates were prepared by inkjet printing with different printing resolution and thermal sintering at different temperatures. Each group contains six samples. Before printing, each piece of silk/epoxy composite film was attached on a glass slide by double sticky tapes. The surfaces of on silk/ epoxy composite film substrates were wiped – cleaned by ethanol and blown by compressed air to remove surface contaminates. The substrates were undertaken plasma surface treatment (HENNIKER HPT – 100, 100% power) for 5 min. The designed pattern was inkjet-printed with low (1270 DPI) and high (2540 DPI) printing resolution on pretreated on silk/epoxy composite film substrates respectively, and thermal sintered at room temperature for 12 h in a vacuum evaporation chamber, 80 °C for 2 h in oven, A 120 °C for 2 h in oven and 150 °C for 1 h in oven, respectively, to ensure the printed samples were fully dried.

Characterization (and Evaluation): Fourier-Transform Infrared Spectroscopy (FT-IR): Spectra in the range of 400–4000 cm^1 were recorded by Bruker ALPHA II FT-IR with KBr pellets. Powder X-ray diffraction (XRD): The crystalline structure of powders was measured using STOE STADI Powder X-ray diffraction system with Cu Kα1 (λ = 1.54056 Å) and Cu Kα2 (λ = 1.54439 Å) and data was collected in the range of 10° < 2θ < 80°. Grazing incidence X-ray diffraction (GIXRD): Films were measured using Empyrean X-ray diffraction system with Cu Kα1 (λ = 1.54056 Å) and Cu Kα2 (λ = 1.54439 Å) and data was collected in the range of 10° < 2θ < 80°. Thermogravimetric analysis (TGA): Silver content of the ink was measured using PerkinElmer STA 6000. 46 mg samples were placed in Al_2O_3 pans and heated from 30 °C up to a maximum of 500 °C at a heating range of 10 °C. Scanning electron microscopy (SEM): The surface morphology of films was imaged and analyzed with Jeol JSM 6701 FEG-SEM at an accelerating voltage of 5 kV. The thickness of the printed film was also measured. Energy-dispersive X-ray spectroscopy (EDS): Samples in SEM were also measured with an accelerating voltage of 20 kV and analyzed by the Oxford Instrument EDS system. UV-vis analysis: The UV-vis absorption spectrum of inks stored for different times was collected at the wavelength range from 200 to 600 nm. The measurements were obtained with standard cuvettes of Shimadzu UV-2700, with a background calibration run of deionized water. Electrical conductivity measurements: The electric conductivity of the printed sample was measured through two-probe resistance measurement with PeakTech Digital multimeter 4000 and calculated based on the specimen thickness from SEM measurement. For each type of substrate with the certain printing resolution, six samples were measured for the calculation of the average conductivity. (Figure S12, Supporting Information) Atomic Force Microscope: The overall roughness of the printed sample of room temperature was measured and calculated from the three 3 µm images. The overall roughness of the printed sample of 80 °C was measured and calculated from the 10 µm image. The overall roughness of the printed sample of 120 °C was measured and calculated from the three 3 µm images. The overall roughness of the printed sample of 150 °C was measured and calculated from the 25 µm images. Droplet surface tension measurements: The surface tension of the commercial ink (from HS Electronics Co., Ltd., China) and synthesized ink was measured with KRUSS Drop Shape Analyzer. The needle diameter was 1.250 mm. Camera angle was set to be 2°. Contact angle measurements: The contact angle and spreading of the droplet of the synthesized ink, AP solution, and water on the silk/epoxy composite film and sulfuric paper was observed and measured with KRUSS Drop Shape Analyzer. For each sample, the base line was manually set along the interface of the liquid phase and the substrate. The contact angle was measured and recorded every 10 s, for 2 h.

Supporting Information

Supporting Information is available from the Wiley Online Library or from the author.

Acknowledgements

C.E.K. acknowledged the EPSRC (EP/V027611/1), UCL- Zhejiang University Strategic Partner Funds and Z.X. and H.B. acknowledge the financial support from the National Natural Science Foundation of China (No. 52103149, 22075244). Y.Z. (data curation, formal analysis, investigation – ink synthesis and inkjet printing, writing of original draft – equal lead), Z.X. (formal analysis, investigation – silk/epoxy composite substrate fabrication and stretching test – equal lead). Shreya Mrig is thanked for collecting PXRD data and Leonardo Santoni for NMR investigations. Dr Matt Blunt is thanked for AFM. Lulu Tian is thanked for her assistance at Zhejiang University.

Conflict of Interest

The authors declare no conflict of interest.

Data Availability Statement

The data that support the findings of this study are available from the corresponding author upon reasonable request.

Keywords

conductive films, flexible substrates, inkjet printing, MOD inks, low temperature, silver precursors, stretchable electronics

Received: September 20, 2022
Revised: November 8, 2022
Published online:

[1] P. Kiddee, R. Naidu, M. H. Wong, *Waste Manage.* **2013**, *33*, 1237.
[2] S. Chen, M. Su, C. Zhang, M. Gao, B. Bao, Q. Yang, B. Su, Y. Song, *Adv. Mater.* **2015**, *27*, 3928.
[3] H. Sirringhaus, T. Kawase, R. H. Friend, T. Shimoda, M. Inbasekaran, W. Wu, E. P. Woo, *Science* **2000**, *290*, 2123.
[4] S. H. Ko, H. Pan, C. P. Grigoropoulos, C. K. Luscombe, J. M. J. Fréchet, D. Poulikakos, *Nanotechnology* **2007**, *18*, 345202.
[5] H. Pan, S. H. Ko, C. P. Grigoropoulos, *Appl. Phys. Lett.* **2008**, *93*, 234104.
[6] S. H. Ko, H. Pan, D. Lee, C. P. Grigoropoulos, H. K. Park, *Jpn. J. Appl. Phys.* **2010**, *49*, 05EC03.
[7] J. Kwon, H. Cho, H. Eom, H. Lee, Y. D. Suh, H. Moon, J. Shin, S. Hong, S. H. Ko, *ACS Appl. Mater. Interfaces* **2016**, *8*, 11575.
[8] Y. Rosen, M. Grouchko, S. Magdassi, *Adv. Mater. Interfaces* **2015**, *2*, 1400448.
[9] Y.-K. Liu, M.-T. Lee, *ACS Appl. Mater. Interfaces* **2014**, *6*, 14576.
[10] C. E. Knapp, J.-B. Chemin, S. P. Douglas, D. A. Ondo, J. Guillot, P. Choquet, N. D. Boscher, *Adv. Mater. Technol.* **2018**, *3*, 1700326.
[11] B. Kang, S. Ko, J. Kim, M. Yang, *Opt. Express* **2011**, *19*, 2573.
[12] C. E. Knapp, E. A. Metcalf, S. Mrig, C. Sanchez-Perez, Samuel. P. Douglas, P. Choquet, N. D. Boscher, *ChemistryOpen* **2018**, *7*, 850.
[13] C. Schoner, A. Tuchscherer, T. Blaudeck, S. F. Jahn, R. R. Baumann, H. Lang, *Thin Solid Films* **2013**, *531*, 147.
[14] J. R. Rumble, *CRC Handbook of Chemistry and Physics.*, CRC Press-Taylor& Francis, United States **2022**.
[15] M. Matsubara, T. Yonezawa, T. Minoshima, H. Tsukamoto, Y. Yong, Y. Ishida, M. T. Nguyen, H. Tanaka, K. Okamoto, T. Osaka, *RSC Adv.* **2015**, *5*, 102904.
[16] Y. Choi, K. Seong, Y. Piao, *Adv. Mater. Interfaces* **2019**, *6*, 1901002.
[17] S. P. Douglas, C. E. Knapp, *ACS Appl. Mater. Interfaces* **2020**, *12*, 26193.
[18] K. R. Zope, D. Cormier, S. A. Williams, *ACS Appl. Mater. Interfaces* **2018**, *10*, 3830.
[19] A. L. Dearden, P. J. Smith, D.-Y. Shin, N. Reis, B. Derby, P. O'Brien, *Macromol. Rapid Commun.* **2005**, *26*, 315.
[20] S. F. Jahn, T. Blaudeck, R. R. Baumann, A. Jakob, P. Ecorchard, T. Rüffer, H. Lang, P. Schmidt, *Chem. Mater.* **2010**, *22*, 3067.
[21] M. Lin, H. Hu, S. Zhou, S. Xu, *Nat. Rev. Mater.* **2022**, *7*, 850.
[22] M. L. Hammock, A. Chortos, B. C.-K. Tee, J. B.-H. Tok, Z. Bao, *Adv. Mater.* **2013**, *25*, 5997.
[23] J. C. Yang, J. Mun, S. Y. Kwon, S. Park, Z. Bao, S. Park, *Adv. Mater.* **2019**, *31*, 1970337.
[24] S. B. Walker, J. A. Lewis, *J. Am. Chem. Soc.* **2012**, *134*, 1419.

[25] M. Vaseem, S.-K. Lee, J.-G. Kim, Y.-B. Hahn, *Chem. Eng. J.* **2016**, *306*, 796.
[26] K. S. Bhat, U. T. Nakate, J.-Y. Yoo, Y. Wang, T. Mahmoudi, Y.-B. Hahn, *Chem. Eng. J.* **2019**, *373*, 355.
[27] H. R. Tinker, M. A. Bhide, E. Magliocca, T. S. Miller, C. E. Knapp, *J. Mater. Sci.* **2021**, *56*, 6966.
[28] Z. Xu, M. Wu, W. Gao, H. Bai, *Adv. Mater.* **2020**, *32*, 2002695.
[29] J. A. Manson, E. H. Chiu, *J. Polym. Sci., Part C: Polym. Symp.* **2007**, *41*, 95.
[30] M. R. H. Siddiqui, S. Alshehri, I. K. Warad, N. M. A. El-Salam, R. M. Mahfouz, *Iran J Med Sci* **2010**, *11*, 3600.
[31] B. M. Abu-Zied, A. M. Asiri, *Thermochim. Acta* **2014**, *581*, 110.
[32] M. Schreck, R. Deshmukh, E. Tervoort, M. Niederberger, *Chem. Mater.* **2022**, *34*, 43.
[33] Y. Bai, C. B. Williams, *Mater. Des.* **2018**, *147*, 146.
[34] H. Khan, J. T. Fell, G. S. Macleod, *Int. J. Pharm.* **2001**, *227*, 113.
[35] M. Grouchko, A. Kamyshny, C. F. Mihailescu, D. F. Anghel, S. Magdassi, *ACS Nano* **2011**, *5*, 3354.
[36] P.-S. Shin, Y.-M. Baek, J.-H. Kim, H.-S. Park, D.-J. Kwon, J.-H. Lee, M.-Y. Kim, K. L. DeVries, J.-M. Park, *Colloids Surf. A* **2018**, *544*, 68.
[37] S. J. Marshall, S. C. Bayne, R. Baier, A. P. Tomsia, G. W. Marshall, *Dent. Mater.* **2010**, *26*, e11.
[38] Z. Huang, M. Su, Q. Yang, Z. Li, S. Chen, Y. Li, X. Zhou, F. Li, Y. Song, *Nat. Commun.* **2017**, *8*, 14110.
[39] M. Su, Z. Huang, Y. Li, X. Qian, Z. Li, X. Hu, Q. Pan, F. Li, L. Li, Y. Song, *Adv. Mater.* **2018**, *30*, 1703963.
[40] H. M. Lee, S.-Y. Choi, A. Jung, S. H. Ko, *Angew. Chem., Int. Ed.* **2013**, *52*, 7718.
[41] H. M. Lee, H. B. Lee, D. S. Jung, J.-Y. Yun, S. H. Ko, S. B. Park, *Langmuir* **2012**, *28*, 13127.